Hydration shell effects in ac-driven single-molecule junctions

Gregor Gurski [1], Henning Kirchberg,[2] Peter Nalbach [3], and Michael Thorwart [1]

[1]*I. Institut für Theoretische Physik, Universität Hamburg, Notkestraße 9, 22607 Hamburg, Germany*
[2]*Department of Chemistry, University of Pennsylvania, Philadelphia, Pennsylvania 19104, USA*
[3]*Fachbereich Wirtschaft & Informationstechnik, Westfälische Hochschule, Münsterstraße 265, 46397 Bocholt, Germany*

We propose a quantum-mechanical model to calculate the current through a single molecular junction immersed in a solvent and surrounded by a thin shell of bound water under an applied ac voltage. The solvent plus hydration shell are captured by a dielectric continuum model for which the resulting spectral density is determined. Here the dielectric properties, e.g., the Debye relaxation time and the dielectric constant, of the bulk solvent and the hydration shell as well as the shell thickness directly enter. We determine the charge current through the molecular junction under an ac voltage in the sequential tunneling regime where we solve a quantum master equation by a real-time diagrammatic technique. Interestingly, the Fourier components of the charge current show an exponential-like decline when the hydration shell thickness increases. Finally, we apply our findings to binary solvent mixtures with varying volume fractions and find that the current is highly sensitive to both the hydration shell thickness as well as the volume fraction of the solvent mixture, giving rise to possible applications as shell and concentration sensors on the molecular scale.

I. INTRODUCTION

The miniaturization of electronic devices remains an enormous challenge. To this end, the field of molecular electronics has made considerable progress in recent years, to where it is now routinely possible to wire an organic molecule, an object as small as 1 nm, between two metallic leads and measure its electronic transport characteristics [1]. Moreover, such single molecular junctions provide a unique platform for simultaneous investigation, manipulation, detection, and stimulation of chemical reactions [2]. Single-molecule junctions have been realized as rectifiers [3], transistors [4], switches [5], sensors [6,7], and have recently attracted much attention due to their promising thermoelectric properties [8–10]. For the experimental investigation of electron transport properties, single-molecule junctions are usually immersed in solution. The inclusion of the bridging molecule into the (bulk) solvent alters the interacting network between the solvent molecules in proximity of the introduced molecule. Thus the solvent molecules must build stronger bonds among each other and/or the junction molecule and form a solvation shell with distinct properties different from the bulk solvent [11–13]. Therefore, not only the type of the surrounding solvent can play a significant role on the transport properties [14–16], but also the formation of a solvation shell can drastically change the electronic conductance of a metal-molecule-metal junction by up to two orders of magnitude [17].

Theoretical description of the influence of the solvent on the transmission properties has relied on utilizing density functional theory (DFT) calculations for the molecular orbitals when placing few, i.e., one to two, water molecules in the vicinity of the bridging molecule [17]. Their rigorous but calculationally involved outcomes have predicted the influence of polar solvents and the hydration shell on the charge transmission through molecular junctions [17,18]. Contrary to these numerically expensive calculations, we were able to provide a theoretical model in our previous work [19] based on a few coarse-grained solvent parameters like the dielectric properties to determine the role of a solvent, and mixtures thereof, on charge transport properties of a molecular junction. There, we found a very good agreement between our calculations and experimentally determined conductance data of a molecular junction.

In the present work, we extend the previous model where the electron transmission is described by incoherent charge-hopping steps by additionally incorporating a hydration shell surrounding the bridging molecule. We show that the influence of the hydration shell on the electric current can be captured by a spectral density where the shell properties, i.e., its thickness or its dielectric function, directly enter. Moreover, we keep the focus on the linear transport regime (linear response to a small external potential) where, from an experimental perspective, it should be easier to distinguish solvent and hydration shell effects from nonlinear effects like the negative differential resistance due to the interplay between two conduction channels accessible by a finite applied dc voltage. To this end we use a different control parameter than the applied dc voltage to study the influence of the solvent with and without hydration shell. Exploiting a quantum-mechanical master equation, we calculate the electric current across the junction in dependence of the frequency of an applied ac voltage. Interestingly, the Fourier components of the charge current for different applied ac voltage frequencies portray a nonlinear behavior when altering the thickness of the hydration shell. We finally propose a valid means to determine the thickness of the shell through the current. An application of a molecular junction acting as a sensor model under an applied ac drive measuring the volume fraction of a binary solvent mixture concludes our paper.
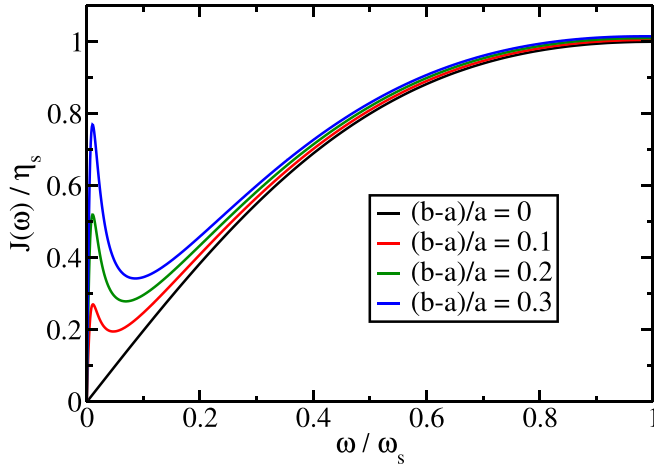
FIG. 1. Spectral density $J(\omega)$ normalized to the reorganization energy η_s of bulk water as a function of the frequency ω (normalized to the cut-off frequency of water ω_s) for various relative hydration shell thicknesses as indicated. The cut-off frequency of the hydration shell is $\omega_{bw} = 10^{-2}\omega_s$.

FIG. 2. First Fourier component of the stationary current $I^{k=1}$ as a function of the ac frequency ω_{ac} in the absence of a solvent (gray dashed line) and for water with various relative hydration shell thicknesses (solid lines) as indicated. Parameters are $a = 5$ Å, $\Delta\mu = 5$ D, $T = 10\,\Gamma$, $\varepsilon_d = 0\,\Gamma$, $eV_{ac} = 10\,\Gamma$, and $\Gamma = 2.5$ meV.

II. MODEL

We consider a metal-molecule-metal junction immersed in a polar solvent plus hydration shell which can be described by the time-dependent Hamiltonian

$$H(t) = H_{mol} + H_{leads}(t) + H_{solv} + H_{mol-solv} + H_{tun},$$

$$H_{mol} = \varepsilon_d d^\dagger d,$$

$$H_{leads}(t) = \sum_{k,r=R,L} (\varepsilon_{k,r}(t) - \mu_r)c_{k,r}^\dagger c_{k,r},$$

$$H_{tun} = \sum_{k,r=R,L} (t_{k,r}c_{k,r}^\dagger d + \text{H.c.}), \tag{1}$$

where the operator d annihilates an electron on the molecule with energy ε_d, and $c_{k,r}$ annihilates an electron in the left ($r = L$) and right ($r = R$) lead, which is held at the chemical potential μ_r (see inset of Fig. 2 for a sketch). The ac voltage is explicitly included in the energies of the lead electrons $\varepsilon_{k,r}(t) = \varepsilon_{k,r} + eV_r \cos(\omega_{ac}t)$, with amplitude $V_L = -V_R = V_{ac}$ and frequency ω_{ac}, respectively. We limit our consideration to two molecular electronic states describing an oxidized state with N and a reduced state with $N + 1$ electrons on the molecule. This standard assumption of strong Coulomb repulsion pushes states with other electronic occupations in energy regimes that are not accessible under the experimental conditions [15,20].

The tunneling hybridization between the molecular level and the corresponding lead r is given by $\Gamma_r = 2\pi|t_{k,r}|^2 D(\varepsilon_F)$, where we assume as usual an energy-independent density of electronic states $D(\varepsilon_F)$ around the Fermi energy $\varepsilon_F \equiv 0$ within both leads (wide-band approximation). We investigate the linear transport regime, i.e., we fix the dc voltage to $\mu_L = \mu_R = eV_{dc} = 0$, and the two tunneling barriers are assumed equal, i.e., $\Gamma_L = \Gamma_R = \Gamma$. Furthermore, we set $\hbar \equiv 1$ and $k_B \equiv 1$.

The polar solvent plus hydration shell is described by its polarization modes with frequency ω_m created by the bosonic

operator $a_m^\dagger$, which gives rise to the Hamiltonian [21,22]

$$H_{solv} = \sum_m \omega_m a_m^\dagger a_m. \tag{2}$$

The polarization modes couple to the electronic occupation of the molecule, with the interaction Hamiltonian

$$H_{mol-solv} = \sum_m g_m d^\dagger d(a_m^\dagger + a_m). \tag{3}$$

The parameter g_m denotes the molecule-solvent plus hydration shell coupling strength for each mode m individually. The couplings between the molecule and the solvent as well as between the molecule and the leads can each be eliminated by a canonical transformation that leads to a renormalization of the parameter ε_d and the tunneling matrix elements $t_{k,r}(t) = t_{k,r} \exp[-i\int_{t_0}^t dt' eV_r \cos(\omega_{ac}t')]$ (see Supplemental Material [23] for more details). From here on we refer to the renormalized parameter as ε_d. The molecule-solvent plus hydration shell coupling is usually administered by the collective spectral density [21,22],

$$J(\omega) = \sum_m g_m^2 \delta(\omega - \omega_m). \tag{4}$$

In the following we use a continuous Debye form of $J(\omega)$ which describes the dielectric properties of the solvent within the Onsager model of quantum solvation [24–26]. By this, the relevant solvent characteristics enters via its dielectric constants and the Debye relaxation time.

III. SPECTRAL DENSITY FOR THE HYDRATION SHELL

We assume that the electronic charge distribution of the molecule is located inside a spherical Onsager cavity with radius a (inset of Fig. 2), which reflects the size of the molecule, and with the vacuum dielectric constant of 1 [27]. The cavity is surrounded by a hydration shell of bound water with outer radius b. This reflects the altered intermolecular-bond network in the vicinity of the bridging molecule. Furthermore,

the occupied and the empty molecular state are, for ease of the analysis, assumed to have dipole moments of different magnitude pointing in the same direction. We assume that the molecule adjusts its dipole moment when an excess electron enters or leaves the molecular junction due to changes of the overall molecular charge density. The resulting molecular dipole polarizes the solvent which induces a backaction (or reaction) electric field inside the cavity. This reaction field interacts with the dipole and mediates the leading coupling between the molecule and the solvent. Although this model, which is based on the Onsager model, does not include the microscopic details of the solvent, it captures the essential low-energy physics of the solvation process in the regime of long polarization wavelengths [21,22,24]. By assuming that the hydration shell is thin compared to the radius of the inner sphere, we perform a Taylor expansion in the relative shell thickness $(b-a)/a$, which yields the spectral density [25,28]

$$J(\omega) = J_s(\omega) + J_{\mathrm{bw}}(\omega), \tag{5}$$

where the first term, $J_s(\omega)$, represents the spectral density of the molecule surrounded by a bulk solvent without hydration shell. The second term, $J_{\mathrm{bw}}(\omega)$, describes the contribution to the spectral density due to the hydration shell of bound water. In the limit of small shell thicknesses, both of the terms can be written in Debye form [25,28] as

$$J_i(\omega) = 2\eta_i \frac{\omega\omega_i}{(\omega^2 + \omega_i^2)}. \tag{6}$$

Here, $\omega_i = \frac{2\varepsilon_{i,S}+1}{2\varepsilon_{i,\infty}+1}\tau_i^{-1}$ is the characteristic cutoff frequency, where $\varepsilon_{i,\infty}$ and $\varepsilon_{i,S}$ are the high- and low- (static) frequency dielectric constants, respectively, and τ_i is the Debye relaxation time. The reorganization energy η is related to the spectral density via [29] $\eta = \int_0^\infty d\omega J(\omega)/\omega$, and for the two contributing parts can be calculated [25,28] as

$$\eta_s = \frac{3(\Delta\mu)^2}{4\pi\varepsilon_0 a^3} \frac{2(\varepsilon_{s,S} - \varepsilon_{s,\infty})}{(2\varepsilon_{s,S}+1)(2\varepsilon_{s,\infty}+1)}, \tag{7}$$

$$\eta_{\mathrm{bw}} = \frac{3(\Delta\mu)^2}{4\pi\varepsilon_0 a^3} \frac{(b-a)}{a} \frac{(\varepsilon_{\mathrm{bw},S}^2 + 2\varepsilon_{s,S}^2)(\varepsilon_{\mathrm{bw},S} - \varepsilon_{\mathrm{bw},\infty})}{\varepsilon_{\mathrm{bw},S}^2 (2\varepsilon_{s,S}+1)^2}, \tag{8}$$

where ε_0 is the vacuum permittivity, a is the radius of the Onsager sphere, b is the radius of the hydration shell, and $\Delta\mu$ is the change in magnitude of the dipole moment from the oxidized to the reduced state. From generic considerations [25,28], one typically expects that $\varepsilon_{s,S} \gg \varepsilon_{s,\infty}$, $\varepsilon_{\mathrm{bw},S} \gg \varepsilon_{\mathrm{bw},\infty}$, $\varepsilon_{s,S} \gg \varepsilon_{\mathrm{bw},S}$, and $\tau_{\mathrm{bw}} \gg \tau_s$, since the solvent molecules are stronger bound in the solvation shell. Hence, we set $\tau_{\mathrm{bw}} = 10\tau_s$ and obtain

$$\eta_{\mathrm{bw}} \approx \frac{\varepsilon_{s,\infty}}{\varepsilon_{\mathrm{bw},S}} \frac{b-a}{a} \eta_s. \tag{9}$$

In Fig. 1 we show an exemplary plot of the spectral density for water with various relative hydration shell thicknesses. The two contributions to the spectral density can be clearly observed by the two separated peaks when the hydration shell is present (colored lines). Without the hydration shell only one peak appears at the cut-off frequency of the bulk water (black line). Therefore an increase in the shell thickness

only increases the bound water part of the spectral density, which in this case has its peak at $\omega_{\mathrm{bw}} = 10^{-2}\omega_s$. Interestingly, one observes a strong impact on $J(\omega)$ already in the limit $(b-a)/a \ll 1$ which signals the electrodynamically collective response of the strongly bound water in the shell. Clearly, as follows from Eq. (9), the slope of $J(\omega)$ at low frequencies depends linearly on the relative hydration shell thickness $(b-a)/a$.

IV. FOURIER COMPONENTS OF THE CURRENT UNDER AC DRIVE

The charge current in the lead $r = L, R$ is given by the time-dependent change of the number of (elementary) charges $e > 0$ as $\langle I_r(t)\rangle = e\frac{d}{dt}\langle N_r(t)\rangle = ie\langle[H_{tun}, N_r](t)\rangle$, where $N_r = \sum_k c_{k,r}^\dagger c_{k,r}$, which is equivalent to

$$\langle I_r(t)\rangle = -ie \sum_k (t_{k,r}(t)\langle c_{k,r}^\dagger(t)d(t)\rangle - t_{k,r}^*(t)\langle d^\dagger(t)c_{k,r}(t)\rangle). \tag{10}$$

Here, $\langle\cdots\rangle$ indicates the expectation value as the trace over all molecule, solvent, and lead degrees of freedom. The explicit time dependence of the tunneling matrix elements $t_{k,r}(t) = t_{k,r}\exp[-i\int_{t_0}^t dt' eV_r\cos(\omega_{ac}t')]$ stems from the time-dependent external ac voltage, which is compressed into the effective tunneling element by a polaron transformation (see Supplemental Material [23] for more details).

Using a quantum master equation according to Refs. [30–32], we obtain

$$\langle I_r(t)\rangle = -e \sum_{\psi_1'\psi_2'\psi_3} \int_{t_0}^t dt' P_{\psi_2'}^{\psi_1'}(t') \Sigma_{\psi_2'\psi_3}^{I_r \psi_1'\psi_3}(t', t), \tag{11}$$

with the matrix element of the reduced density operator of the molecule $P_{\psi_2}^{\psi_1}(t) = \langle\psi_1|\rho_{mol}(t)|\psi_2\rangle$. Here, $|\psi_i\rangle$ are the reduced and oxidized eigenstates of the molecule, i.e., $H_{mol}|\psi_i\rangle = \varepsilon_{\psi_i}|\psi_i\rangle$, and the irreducible self-energy $\Sigma_{\psi_2'\psi_3}^{I_r \psi_1'\psi_3}(t', t)$ describes possible charge migration processes between the molecule and the leads while interacting with the solvent (see Supplemental Material [23] for more details). We exploit the Markov approximation by assuming that all solvent relaxation processes are fast between two subsequent charge migration processes, so that we neglect memory effects for the electron $\rho_{mol}(t') \simeq \rho_{mol}(t)$. In this sequential tunneling regime, the irreducible self-energy consists of four summands of similar form such as

$$\Sigma_{\psi_2'\psi_3}^{I_r \psi_1'\psi_3}(t', t) = i\frac{\Gamma}{2\beta}\langle\psi_3|d|\psi_1'\rangle\langle\psi_2'|d^\dagger|\psi_3\rangle \sum_{q,p} e^{ip\omega_{ac}t}$$

$$\times J_q\left(\frac{eV_r}{\omega_{ac}}\right) J_{q-p}\left(\frac{eV_r}{\omega_{ac}}\right) e^{i\mu_r(t-t'-\frac{i}{B})}$$

$$\times \frac{e^{i(\varepsilon_{\psi_1'} - \varepsilon_{\psi_3} + (q-p)\omega_{ac})(t-t')} e^{-W(t-t')}}{\sinh\left[\frac{\pi}{\beta}\left(t-t'-\frac{i}{B}\right)\right]} + \cdots, \tag{12}$$

where B is the bandwidth of accessible electronic states in the metal leads (see Supplemental Material [23] for more details), and $\beta = T^{-1}$ is the inverse thermal energy. We describe the

ac voltage in Eq. (12) by a Jacobi-Anger expansion in its modes (here q and p) referred to as photon sidebands [33,34], which correspond to photon (energy quantum) emission and absorption processes, where $J_q(x)$ are the Bessel functions of the first kind; see also the Tien-Gordon model of a microwave field [35]. The exponent $W(t)$ is found to be [30–32]

$$W(t) = \int_0^\infty \frac{d\omega}{\pi} \frac{J(\omega)}{\omega^2} \left[[1 - \cos(\omega t)] \coth\left(\frac{\beta\omega}{2}\right) + i \sin(\omega t) \right],$$
(13)

where $J(\omega)$ is the spectral density of the bulk solvent plus hydration shell. The Fourier transform $P^\pm(\omega) = \frac{1}{2\pi} \int dt\, e^{i\omega t} e^{W(\pm t)}$ describes the probability that an electron absorbs (P^+) or emits (P^-) the boson energy ω [30–32]. With the Markov approximation we can directly calculate the time integral from Eq. (11) and find for the irreducible self-energy in the stationary limit, i.e., for $t_0 \to -\infty$, that $\Sigma_{\psi_2'\psi_3}^{I_r\psi_1'\psi_3}(t) = \int_{t_0}^t dt' \Sigma_{\psi_2'\psi_3}^{I_r\psi_1'\psi_3}(t', t) = \sum_p \Sigma_{\psi_2'\psi_3}^{I_r\psi_1'\psi_3, p} e^{ip\omega_{ac}t}$. We use the periodicity of this expression of the irreducible self-energy and Fourier expand the matrix element of the reduced density operator of the molecule, i.e., $P_{\psi_2}^{\psi_1}(t) = \sum_k P_{\psi_2}^{\psi_1, k} e^{ik\omega_{ac}t}$. The Fourier components $P_{\psi_2}^{\psi_1, k}$ are calculated by solving the master equation in Fourier space (see Supplemental Material [23] for more details).

Finally, we obtain the stationary current

$$\langle I_r(t) \rangle = -e \sum_{\psi_1'\psi_2'\psi_3} P_{\psi_2'}^{\psi_1'}(t) \Sigma_{\psi_2'\psi_3}^{I_r\psi_1'\psi_3}(t)$$

$$= -e \sum_{\psi_1'\psi_2'\psi_3} \sum_{kq} P_{\psi_2'}^{\psi_1', q} \Sigma_{\psi_2'\psi_3}^{I_r\psi_1'\psi_3, k-q} e^{ik\omega_{ac}t}$$

$$= \sum_k I_r^k e^{ik\omega_{ac}t},$$
(14)

where, in the last line, the current under the applied ac voltage is written in the form of a Fourier expansion where the Fourier components are given by

$$I_r^k = -e \sum_{\psi_1'\psi_2'\psi_3} \sum_q P_{\psi_2'}^{\psi_1', q} \Sigma_{\psi_2'\psi_3}^{I_r\psi_1'\psi_3, k-q}.$$
(15)

This result is used to investigate the influence of the solvent and different extensions of the hydration shell on the current under an applied ac voltage. In the following we set the molecule-lead coupling $\Gamma = 2.5$ meV so that a temperature of $T = 10\,\Gamma$ corresponds to room temperature (300 K). Additionally, we consider a realistic molecular radius $a = 5$ Å and a typical dipole moment change of $\Delta\mu = 5$ D [36–41].

V. RESULTS AND DISCUSSION

In order to investigate the influence of the hydration shell as well as the bulk water on the tunneling current, we use an ac voltage with amplitude $eV_{ac} = 10\,\Gamma$ and calculate the Fourier components of the stationary current as a function of the ac frequency ω_{ac}. Due to the fact that we are in the linear transport regime with $V_{dc} = 0$, the zeroth Fourier component of the current vanishes since it corresponds to the dc current. Given the symmetry of our model where the leads' Fermi level

align with the molecular level in the absence of an applied voltage, all even Fourier components of the ac current vanish and only the odd ones are nonzero. In Fig. 2 we show the first Fourier component $I^{k=1}$ of the stationary current, both in the absence of a solvent and for water, with various relative hydration shell thicknesses (see Supplemental Material [23] for the next nonvanishing Fourier component). $I^{k=1}$ is only induced by the applied ac voltage so that in the limit $\omega_{ac}/\Gamma \to 0$ no potential difference can be built up across the molecule in the relevant charge transfer timescale Γ^{-1} and $I^{k=1}$ goes to zero. The $I^{k=1}$-ω_{ac} curve goes through a maximum close to the frequency $\omega_{ac} = eV_{ac} = 10\,\Gamma$, which can be attributed to the Bessel functions appearing in Eq. (12), because the product of the zeroth and first Bessel function is maximal when the argument eV_{ac}/ω_{ac} is close to 1. These two Bessel functions are the main contributors to the first Fourier component of the stationary current for frequencies at or above $\omega_{ac} = eV_{ac}$, because all higher Bessel functions are significantly smaller in that frequency range. Put differently, the energy supplied by the ac voltage $(\hbar)\omega_{ac}$ matches the electric energy eV_{ac} by the (time-dependent) voltage sweep across the molecule. Higher ac frequencies ω_{ac} lead to an energetic mismatch and $I^{k=1}$ declines. Similar observations are found in the photon-assisted current in single molecular junctions where $I^{k=1}$ is the related current induced when electrons exchange a single energy quantum, i.e., a photon with the oscillating ac field [33].

When water is considered as a solvent surrounding the molecule, then the $I^{k=1}$-ω_{ac} curves significantly decrease, see Fig. 2. This is due to the fact that a part of the electric potential energy of the ac drive is used for the reorganization of the solvent. Even more energy is needed to reorganize the solvent when we additionally consider the hydration shell. That is why the maximum current $I_{max}^{k=1}$ decreases further with an increase of the hydration shell as depicted in Fig. 2. Furthermore, we notice that the $I^{k=1}$ values for different ω_{ac} in a given window ($\sim$10–70 Γ) decline differently when increasing the shell thickness. This behavior reflects the distinct coupling of the molecular level to different polarization modes captured by the spectral density (see Fig. 1).

In Fig. 3(a) we show $I_{max}^{k=1}$ with respect to the relative shell thickness $(b - a)/a$ and observe that it is consistent with an exponential decrease. Such an exponential decrease of $I_{max}^{k=1}$ with respect to the shell thickness could be expected from the real part of $W(t)$ from Eq. (13) where the spectral density $J(\omega)$ enters. The dominant term in $J(\omega)$ is the reorganization energy of the shell, which is directly proportional to its relative thickness $(b - a)/a$ [see Eq. (9)]. Note that deviations from that behavior may occur due to the exact calculations of the time integral over the self-energy in Eq. (11). The decline of $I_{max}^{k=1}$ directly reflects the enhanced collective response of the strongly bound molecules in the hydration shell. Interestingly, the position $\omega_{ac}(I_{max}^{k=1})$ at which $I^{k=1}$ is maximal is also influenced by the shell and shifts to higher frequencies when compared to the case without the hydration shell, see Fig. 3(b). Since the contribution from the irreducible self-energy (12) to the current is maximal when the imaginary part of the exponent vanishes, the observed increase of $\omega_{ac}(I_{max}^{k=1})$ with a growing hydration shell can be related to the increasing

(a) $I_{\max}^{k=1}$ **(b)** $\omega_{ac}(I_{\max}^{k=1})$
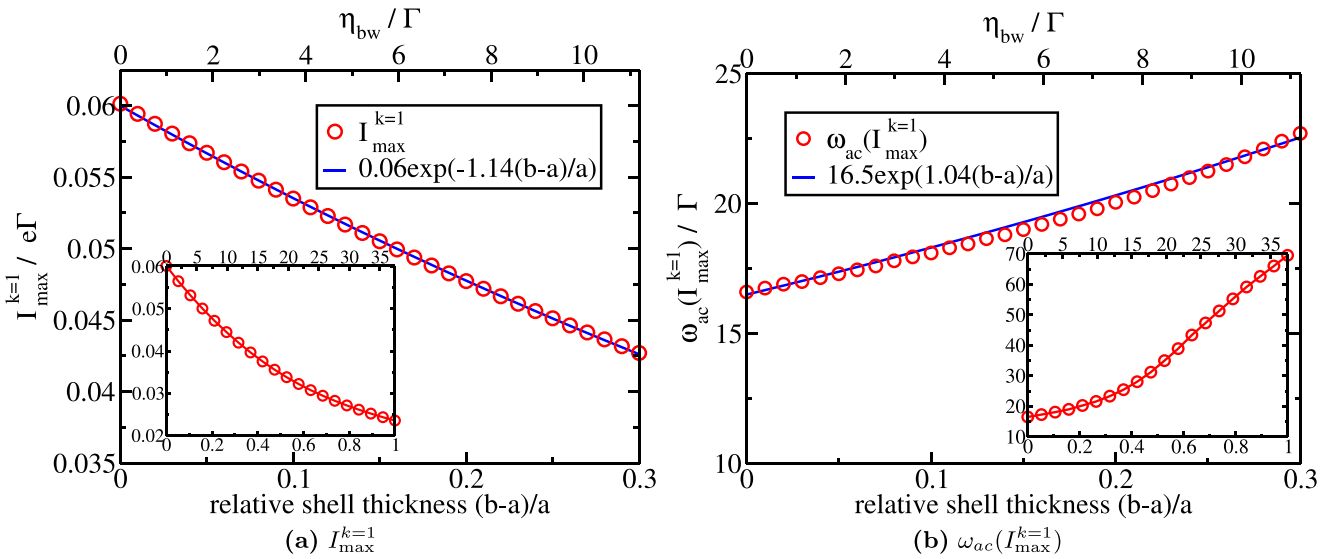
FIG. 3. (a) Maximum of the first Fourier component of the stationary current $I_{\max}^{k=1}$ as a function of the relative shell thickness $(b-a)/a$. (b) Frequency $\omega_{ac}(I_{\max}^{k=1})$ position at $I_{\max}^{k=1}$ as a function of the relative shell thickness $(b-a)/a$. Parameters are $a = 5$ Å, $\Delta\mu = 5$ D, $T = 10\,\Gamma$, $\varepsilon_d = 0\,\Gamma$, $eV_{ac} = 10\,\Gamma$, and $\Gamma = 2.5$ meV. The insets show the trend for larger relative shell thicknesses within the expansion of Eq. (5). The blue lines are fits to exponential functions as indicated.

imaginary part of $W(t)$ in Eq. (13) that makes the imaginary part in the exponent in Eq. (12) smaller.

VI. APPLICATION TO BINARY SOLVENT MIXTURES

In our previous work [19], we have investigated the non-linear differential conductance G in a molecular junction under an applied dc voltage as a function of the volume fraction f for the binary mixtures between butanol and ethanol, chlorobenzene and nitrobenzene, as well as toluene and nitrobenzene. With the same methodology as in Sec. IV, we now investigate the first-order Fourier component $I^{k=1}$ under an ac voltage with given frequency and amplitude. Notably, we find the same qualitative behavior for $I^{k=1}$ with respect to f, Fig. 4, as for the nonlinear differential conductance. $I^{k=1}$ and G in Ref. [19] are highly influenced by the volume fraction f of the additional solvent. The $I^{k=1}$-f (G-f in [19]) behavior depends on the specific binary mixture and reflects nonmonotonous characteristics of the dielectric function (see Eq. (6) in Ref. [19]),

$$\varepsilon(\omega) = (1-f)\varepsilon_h(\omega) + f\varepsilon_i(\omega), \qquad (16)$$

which includes the relative concentrations of a host $(1-f)$ and an inclusive (f) solvent, with the dielectric permittivity $\varepsilon_h(\omega)$ and $\varepsilon_i(\omega)$, respectively. In both cases this dielectric function enters in the same functional way into the spectral density, leading to a sum of two contributions as in Eq. (5). The main difference is that we are now in the linear transport regime and still find that $I^{k=1}$ is highly sensitive to both the volume fraction and the individual solvents themselves.

VII. CONCLUSIONS

We present a theory to calculate the charge current under an ac voltage through a molecular junction surrounded

by a polar solvent plus a hydration shell. We have used a quantum-mechanical real-time diagrammatic technique in the regime of sequential charge tunneling, which includes the electrostatic molecule-solvent plus hydration shell coupling in the single electron transfer nonperturbatively. Under ac drive we focus on the Fourier components of the current in the linear transport regime. By variation of the ac frequency we
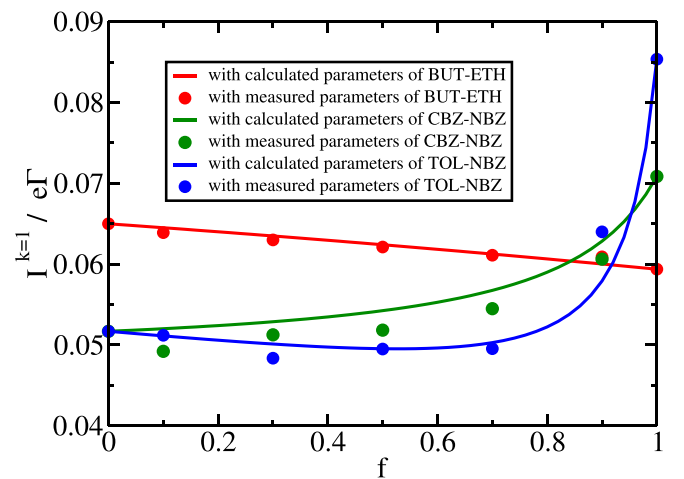
FIG. 4. First Fourier component of the stationary current as a function of the volume fraction f for the binary mixtures between butanol and ethanol, chlorobenzene and nitrobenzene, as well as toluene and nitrobenzene. The solid lines show the results calculated using the effective dielectric parameters of Gladstone-Dale in an effective Debye spectral density [19]. In addition, the circles mark the current calculated with a single Debye spectral density of the mixture with the directly measured dielectric parameters taken from Ref. [42]. Parameters are $a = 5$ Å, $b = 0$, $\Delta\mu = 5$ D, $T = 10\,\Gamma$, $\varepsilon_d = 0\,\Gamma$, $eV_{ac} = 10\,\Gamma$, $\omega_{ac} = 10\,\Gamma$, and $\Gamma = 2.5$ meV.

find a sensitive impact of the thickness of the hydration shell around the molecule on the first Fourier component of the current. We use the approach by Gilmore and McKenzie [28] to determine the effective spectral density of the solvent plus hydration shell. Here, the dielectric properties, i.e., dielectric constants and Debye relaxation time, of the solvent and the shell directly enter. We find that by comparing the results of no solvent and water as a solvent both with and without hydration shell we can determine the thickness of the shell through the current under ac drive. The relative shell thickness can be read off, for example, by the exponential-like decline of the first Fourier component of the current. Another possible application is given by a prototype molecular junction under ac drive, measuring the volume fraction of a binary solvent mixture. Therefore the proposed theoretical methodology may be applied for a molecular sensor to determine the thickness of a hydration shell or the volume fraction of a solvent mixture with high sensitivity.

[1] F. Evers, R. Korytár, S. Tewari, and J. M. van Ruitenbeek, Advances and challenges in single-molecule electron transport, Rev. Mod. Phys. **92**, 035001 (2020).

[2] I. Bunker, R. T. Ayinla, and K. Wang, Single-molecule chemical reactions unveiled in molecular junctions, Processes **10**, 2574 (2022).

[3] X. Qiu, S. Rousseva, G. Ye, J. C. Hummelen, and R. C. Chiechi, In operando modulation of rectification in molecular tunneling junctions comprising reconfigurable molecular self-assemblies, Adv. Mater. **33**, 2006109 (2021).

[4] H. Park, J. Park, A. K. Lim, E. H. Anderson, A. P. Alivisatos, and P. L. McEuen, Nanomechanical oscillations in a single-C 60 transistor, Nature (London) **407**, 57 (2000).

[5] S. Y. Quek, M. Kamenetska, M. L. Steigerwald, H. J. Choi, S. G. Louie, M. S. Hybertsen, J. Neaton, and L. Venkataraman, Mechanically controlled binary conductance switching of a single-molecule junction, Nat. Nanotechnol. **4**, 230 (2009).

[6] S.-L. Lv, C. Zeng, Z. Yu, J.-F. Zheng, Y.-H. Wang, Y. Shao, and X.-S. Zhou, Recent advances in single-molecule sensors based on STM break junction measurements, Biosensors **12**, 565 (2022).

[7] Z. Li, M. Smeu, S. Afsari, Y. Xing, M. A. Ratner, and E. Borguet, Single-molecule sensing of environmental pH—An STM break junction and NEGF-DFT approach, Angew. Chem. Int. Ed. **53**, 1098 (2014).

[8] J. K. Sowa, J. A. Mol, and E. M. Gauger, Marcus theory of thermoelectricity in molecular junctions, J. Phys. Chem. C **123**, 4103 (2019).

[9] N. A. Zimbovskaya, Seebeck effect in molecular junctions, J. Phys.: Condens. Matter **28**, 183002 (2016).

[10] H. Kirchberg and A. Nitzan, Energy transfer and thermo-electricity in molecular junctions in non-equilibrated solvents, J. Chem. Phys. **156**, 094306 (2022).

[11] H. Kirchberg, P. Nalbach, C. Bressler, and M. Thorwart, Spectroscopic signatures of the dynamical hydrophobic solvation shell formation, J. Phys. Chem. B **123**, 2106 (2019).

[12] D. Laage, T. Elsaesser, and J. T. Hynes, Water dynamics in the hydration shells of biomolecules, Chem. Rev. **117**, 10694 (2017).

[13] H. Kirchberg and M. Thorwart, Time-resolved probing of the nonequilibrium structural solvation dynamics by the time-dependent Stokes shift, J. Phys. Chem. B **124**, 5717 (2020).

[14] K. Luka-Guth, S. Hambsch, A. Bloch, P. Ehrenreich, B. M. Briechle, F. Kilibarda, T. Sendler, D. Sysoiev, T. Huhn, A. Erbe, and E. Scheer, Role of solvents in the electronic transport properties of single-molecule junctions, Beilstein J. Nanotechnol. **7**, 1055 (2016).

[15] Z. Tang, S. Hou, Q. Wu, Z. Tan, J. Zheng, R. Li, J. Liu, Y. Yang, H. Sadeghi, J. Shi *et al.*, Solvent-molecule interaction induced gating of charge transport through single-molecule junctions, Sci. Bull. **65**, 944 (2020).

[16] V. Fatemi, M. Kamenetska, J. Neaton, and L. Venkataraman, Environmental control of single-molecule junction transport, Nano Lett. **11**, 1988 (2011).

[17] E. Leary, H. Höbenreich, S. J. Higgins, H. van Zalinge, W. Haiss, R. J. Nichols, C. M. Finch, I. Grace, C. J. Lambert, R. McGrath, and J. Smerdon, Single-Molecule Solvation-Shell Sensing, Phys. Rev. Lett. **102**, 086801 (2009).

[18] S. Yeganeh, M. Galperin, and M. A. Ratner, Switching in molecular transport junctions: Polarization response, J. Am. Chem. Soc. **129**, 13313 (2007).

[19] G. Gurski, H. Kirchberg, P. Nalbach, and M. Thorwart, Single-molecule junctions sensitive to binary solvent mixtures, Phys. Rev. B **106**, 075413 (2022).

[20] J. Zhang, A. M. Kuznetsov, I. G. Medvedev, Q. Chi, T. Albrecht, P. S. Jensen, and J. Ulstrup, Single-molecule electron transfer in electrochemical environments, Chem. Rev. **108**, 2737 (2008).

[21] A. Nitzan, *Chemical Dynamics in Condensed Phases* (Oxford University Press, Oxford, 2006).

[22] V. May and O. Kühn, *Charge and Energy Transfer Dynamics in Molecular Systems* (Wiley-VCH, Weinheim, 2011).

[23] See Supplemental Material at http://link.aps.org/supplemental/10.1103/PhysRevB.107.165413 for a plot of the third Fourier component of the stationary current and a detailed account to calculate the Fourier components of the current under ac drive.

[24] J. Gilmore and R. H. McKenzie, Spin boson models for quantum decoherence of electronic excitations of biomolecules and quantum dots in a solvent, J. Phys.: Condens. Matter **17**, 1735 (2005).

[25] P. Nalbach, A. Achner, M. Frey, M. Grosser, C. Bressler, and M. Thorwart, Hydration shell effects in the relaxation dynamics of photoexcited fe-ii complexes in water, J. Chem. Phys. **141**, 044304 (2014).

[26] H. Kirchberg, P. Nalbach, and M. Thorwart, Nonequilibrium quantum solvation with a time-dependent Onsager cavity, J. Chem. Phys. **148**, 164301 (2018).

[27] L. Onsager, Electric moments of molecules in liquids, J. Am. Chem. Soc. **58**, 1486 (1936).

[28] J. Gilmore and R. H. McKenzie, Quantum dynamics of electronic excitations in biomolecular chromophores: Role of the protein environment and solvent, J. Phys. Chem. A **112**, 2162 (2008).

[29] C.-P. Hsu, Reorganization energies and spectral densities for electron transfer problems in charge transport materials, Phys. Chem. Chem. Phys. **22**, 21630 (2020).

[30] J. König, H. Schoeller, and G. Schön, Zero-Bias Anomalies and Boson-Assisted Tunneling Through Quantum Dots, Phys. Rev. Lett. **76**, 1715 (1996).

[31] J. König, J. Schmid, H. Schoeller, and G. Schön, Resonant tunneling through ultrasmall quantum dots: Zero-bias anomalies, magnetic-field dependence, and boson-assisted transport, Phys. Rev. B **54**, 16820 (1996).

[32] H. Schoeller, Transport theorie für wechselwirkende quantenpunkte, Habilitation thesis, Karlsruhe Institut für Technologie, 1997.

[33] G. Platero and R. Aguado, Photon-assisted transport in semiconductor nanostructures, Phys. Rep. **395**, 1 (2004).

[34] L. P. Kouwenhoven, S. Jauhar, K. McCormick, D. Dixon, P. L. McEuen, Yu. V. Nazarov, N. C. van der Vaart, and C. T. Foxon, Photon-assisted tunneling through a quantum dot, Phys. Rev. B **50**, 2019(R) (1994).

[35] P. Tien and J. Gordon, Multiphoton process observed in the interaction of microwave fields with the tunneling between superconductor films, Phys. Rev. **129**, 647 (1963).

[36] C. Reichardt and T. Welton, *Solvents and Solvent Effects in Organic Chemistry* (Wiley-VCH Verlag & Co. KGaA, Weinheim, 2011).

[37] L. J. Richter, C. S.-C. Yang, P. T. Wilson, C. A. Hacker, R. D. van Zee, J. J. Stapleton, D. L. Allara, Y. Yao, and J. M. Tour, Optical characterization of oligo(phenylene-ethynylene) self-assembled monolayers on gold, J. Phys. Chem. B **108**, 12547 (2004).

[38] Y. Li, J. Zhao, and G. Yin, Theoretical investigations of oligo(phenylene ethylene) molecular wire: Effects from substituents and external electric field, Comput. Mater. Sci. **39**, 775 (2007).

[39] K. Selvaraju, M. Jothi, and P. Kumaradhas, Exploring the charge density distribution and the electrical characteristics of oligo phenylene ethylene molecular nanowire using quantum chemical and charge density analysis, Comput. Theor. Chem. **996**, 1 (2012).

[40] H. Lissau, R. Frisenda, S. T. Olsen, M. Jevric, C. R. Parker, A. Kadziola, T. Hansen, H. S. J. van der Zant, M. Brøndsted Nielsen, and K. V. Mikkelsen, Tracking molecular resonance forms of donor–acceptor push–pull molecules by single-molecule conductance experiments, Nat. Commun. **6**, 10233 (2015).

[41] R. Frisenda, S. Tarkuc, E. Galan, M. L. Perrin, R. Eelkema, F. C. Grozema, and H. S. J. van der Zant, Electrical properties and mechanical stability of anchoring groups for single-molecule electronics, Beilstein J. Nanotechnol. **6**, 1558 (2015).

[42] J. Lou, T. A. Hatton, and P. E. Laibinis, Effective dielectric properties of solvent mixtures at microwave frequencies, J. Phys. Chem. A **101**, 5262 (1997).